

## Research Article

### Calculation of Temperature Rise in Dry-type Air-core Reactors Using Strong Coupling of Fluid-Temperature Field

<sup>1</sup>Yujiao Zhang, <sup>1</sup>Xiongfeng Huang, <sup>2</sup>Gang Hu, <sup>3</sup>Tao Huang and <sup>3</sup>Jiangjun Ruan

<sup>1</sup>College of Electrical Engineering and New Energy,

<sup>2</sup>College of Computer and Information Technology, China Three Gorges University, Yichang 443002, China

<sup>3</sup>Department of Electrical Engineering, Wuhan University, Wuhan 430072, China

**Abstract:** The ventilation system design of dry-type air-core reactor is a complex task that must determine the thermal loads to achieve the maximum insulation material exploitation. In this study, the temperature rise in reactor is due to Joule's losses and heat dissipation by air convection, convection and radiation. The Joule's losses calculated by coupled magnetic field-circuit analysis are used as the input for the thermal field by finite-element analysis, which is directly coupled with fluid analysis. Finally, the temperature distributions of reactor can be calculated. Therefore, the thermal performance analysis of air-core reactor could be conducted in the early design stage to guarantee the insulation material requirements.

**Keywords:** Coupled magnetic field-circuit, dry-type air-core reactor, finite-element analysis, fluid field, thermal field, temperature rise

## INTRODUCTION

In power system, dry-type air-core reactor is employed to limit current, steady voltage and compensate reactive power. In practical applications, air-core reactor during operation is prone to faults, including partial discharge, overheating and burnout (Liu *et al.*, 2003). In the case of dry-type reactors with fully encapsulated windings, the insulation between turns is usually a solid dielectric material. In selecting appropriate materials to be utilized as turns' insulation on the conductors, it is necessary to evaluate dielectric properties, mechanical properties and aging characteristics under operating conditions. Performance at temperature is one of the main evaluating criteria for materials, so the temperature rise is one of the main aging mechanisms that have to be considered, especially for the overall system (IEEE Std., 1996).

Accurate calculation of the temperature distribution is pivotal to the optimal design, which is a multi-physical coupled process that involves electromagnetic losses as well as fluid dynamic and thermal behavior. In traditional research, the average temperature rise of reactor was calculated by empirical formula (Wu *et al.*, 1997). However, even if average temperature rise satisfies design requirement, the hottest-spot temperature in reactor might exceed the maximum temperature limits of insulation materials. Moreover, thermal field was simulated by finite-element method (FEM) after calculating the heat transfer coefficient by

using Nusselt number (Liu, 1991; Wu *et al.*, 2002; Ho *et al.*, 2006, 2007). Nevertheless, the fluid dynamic behavior cannot be accurately described not by simulating fluid field. The calculation results were very different with the measurement results, so the heat transfer coefficient must be repeatedly modified. Therefore, a coupled analysis of fluid field and thermal field is mandatory to compute the temperature rise in the design stage (Zhang *et al.*, 2012a).

In this study, we calculated temperature distributions by using the coupled magnetic field-circuit method and coupled fluid-dynamical and thermal finite-element analysis in a type of dry-type air-core reactor, as shown in Fig. 1. Through the big ventilation duct, cooling air taken in from the exterior to the interior of reactor by fan is sent to exothermic parts such as the windings. On the top of reactor, there are two layers of rainproof shield for protecting the reactor against rain. A 2-D computational model can be established to analyze the multi-physics simulation due to the axial symmetry. The Joule's losses calculated by the coupled field-circuit analysis are used as the input for the thermal field analysis, which is deeply dependent on accurate air fluid field analysis.

## THEORY AND FORMULATION

**Coupled magnetic field-circuit calculation:** The dry-type air-core reactor contains parallel several



Fig. 1: This type of reactors in substation

encapsulated windings and each of them contains parallel several layers of small-diameter aluminum conductors. The ac voltage, whose frequency is 50 Hz, is applied to the conductor in each layer. In cylindrical coordinate system, the magnetic field equation can be given as Liu *et al.* (2003):

$$\frac{\partial}{\partial r} \left( \frac{1}{r} \frac{\partial A}{\partial r} \right) + \frac{\partial}{\partial z} \left( \frac{1}{r} \frac{\partial A}{\partial z} \right) = -\mu_0 J \quad (1)$$

The terminal voltage of the conductors in the  $i^{\text{th}}$  layer is given as:

$$u = i_i R_i + \frac{d\Psi_i}{dt} \quad (2)$$

$$\Psi_i = N_i \int \nabla_s \times A g dS = N_i \int A_l g dl \quad (3)$$

where,

$\Psi_i$  = The flux linkage of conductors in the  $i^{\text{th}}$  layer

$N_i$  = The number of turns

From Eq. (1-3), the voltage equation can be described with magnetic vector potential ( $A$ ). These equations can be solved by FEM. After obtaining the value of  $A$ , the current can be calculated. Then, Joule's losses can be calculated by Eq. (4).

$$Q = \rho J^2 \quad (4)$$

where,

$\rho$  = Resistivity of aluminum

$J$  = Current density

**Strong coupling of fluid-temperature field calculation:** For the system of the reactor shown in Fig. 1, there are three heat dissipation modes, involving heat conduction, heat convection and thermal radiation.

For the encapsulated windings, the main heat dissipation mode is heat conduction. For the surface between encapsulated windings and surrounding air, the main heat dissipation mode is heat forced convection and thermal radiation. Finally, our concern is the temperature distributions of each encapsulated winding.

- **Heat conduction:** For the encapsulated windings, the steady state heat conduction equation for solid is given as Zhang *et al.* (2012b):

$$\frac{1}{r} \frac{\partial}{\partial r} \left( k \frac{\partial T}{\partial r} \right) + \frac{\partial}{\partial z} \left( k \frac{\partial T}{\partial z} \right) = -Q \quad (5)$$

where,

$k$  = The coefficient of heat conductivity

$Q$  = The heat generation of unit volume in aluminum conductors

- **Heat convection:** The forced convection of air satisfies the Navier-Stokes Equations, which consist of three groups of equations. For two-dimensional incompressible steady fluid, the Navier-Stokes Equations in cylindrical coordinate system can be simplified as following (Wu *et al.*, 2002):

Continuity equation:

$$\frac{1}{r} \frac{\partial (r v_r)}{\partial r} + \frac{\partial v_z}{\partial z} = 0 \quad (6)$$

Momentum conservation equations:

$$\rho \left( v_r \frac{\partial v_r}{\partial r} + v_z \frac{\partial v_r}{\partial z} \right) = -\frac{\partial p}{\partial r} + \mu \left[ \frac{\partial}{\partial r} \left( \frac{1}{r} \frac{\partial (r v_r)}{\partial r} \right) + \frac{\partial^2 v_r}{\partial z^2} \right] \quad (7)$$

$$\rho \left( v_r \frac{\partial v_z}{\partial r} + v_z \frac{\partial v_z}{\partial z} \right) = -\frac{\partial p}{\partial z} + \mu \left[ \frac{1}{r} \frac{\partial}{\partial r} \left( r \frac{\partial v_z}{\partial r} \right) + \frac{\partial^2 v_z}{\partial z^2} \right] \quad (8)$$

Energy equation is given as:

$$\rho c \left( v_r \frac{\partial T}{\partial r} + v_z \frac{\partial T}{\partial z} \right) = k \nabla^2 T + Q \quad (9)$$

where,

$\rho$  = The density of air

$\mu$  = The viscosity coefficient

$p$  = Pressure

$c$  = The specific heat

$T$  = The fluid temperature and  $v_r$  and  $v_z$  are the velocity in the  $r$ - and  $z$ - directions, respectively

Because of the large Reynolds number ( $>2300$ ), the fluid gets turbulent. The standard  $k$ - $\epsilon$  turbulence model was used in the turbulence calculation (Zhang *et al.*, 2012a).

$$\frac{\partial(\rho k)}{\partial t} + \frac{\partial(\rho k u_i)}{\partial x_i} = \frac{\partial}{\partial x_j} \left[ \left( \mu + \frac{\mu_t}{\sigma_k} \right) \frac{\partial k}{\partial x_j} \right] + G_k - \rho \epsilon \quad (10)$$

$$\frac{\partial(\rho \epsilon)}{\partial t} + \frac{\partial(\rho \epsilon u_i)}{\partial x_i} = \frac{\partial}{\partial x_j} \left[ \left( \mu + \frac{\mu_t}{\sigma_\epsilon} \right) \frac{\partial \epsilon}{\partial x_j} \right] + \frac{C_{1\epsilon}}{k} G_k - C_{2\epsilon} \rho \frac{\epsilon^2}{k} \quad (11)$$

$$G_k = \mu_t \left\{ 2 \left[ \left( \frac{\partial u}{\partial x} \right)^2 + \left( \frac{\partial v}{\partial y} \right)^2 + \left( \frac{\partial w}{\partial z} \right)^2 \right] + \left( \frac{\partial u}{\partial y} + \frac{\partial v}{\partial x} \right)^2 + \left( \frac{\partial u}{\partial z} + \frac{\partial w}{\partial x} \right)^2 + \left( \frac{\partial v}{\partial z} + \frac{\partial w}{\partial y} \right)^2 \right\} \quad (12)$$

where,

$G_k$  = The turbulent generation rate  
 $\mu_t = \rho C_\mu (k^2/\epsilon)$  = The viscosity coefficient

As the constants in the equations,  $C_{1\epsilon} = 1.44$ ,  $C_{2\epsilon} = 1.92$ ,  $C_\mu = 0.09$ ,  $\sigma_k = 1.0$ ,  $\sigma_\epsilon = 1.3$ .

- **Radiation:** For a system of two surfaces (surface  $i$  and  $j$ ) radiating to each other, the heat transfer rate between surfaces  $i$  and  $j$  is expressed as Wu *et al.* (2002):

$$Q_{ij} = \sigma \epsilon_i F_{ij} A_i (T_i^4 - T_j^4) \quad (13)$$

where,

- $\sigma$  = Stefan-Boltzmann constant
- $\epsilon_i$  = The effective emissivity of surface  $i$
- $F_{ij}$  = The radiation view factor between surface  $i$  and  $j$
- $A_i$  = The area of surface  $i$  and  $T_i$
- $T_j$  = The absolute temperature of surface  $i$  and  $j$

### CALCULATION AND ANALYSIS

**Structor of reactor:** According to the reactor shown in Fig. 1, the model of overall reactor and the vertical part of ventilation duct is axisymmetric, so a 2-D model is established, as shown in Fig. 2. There are ten encapsulated windings and each of them has their own different size. Moreover, on both sides of each encapsulated winding are wound with four layers of DMD (Dacron Mylar Dacron) and three layers of glass fiber dipped by epoxy. Each layer of aluminum conductor is wound with four layers of polyester film. It means that there are eight layers of polyester film between two layers of aluminum conductor.

**Finite-element model and boundary conditions:** On the basis of model shown in Fig. 2, the finite-element

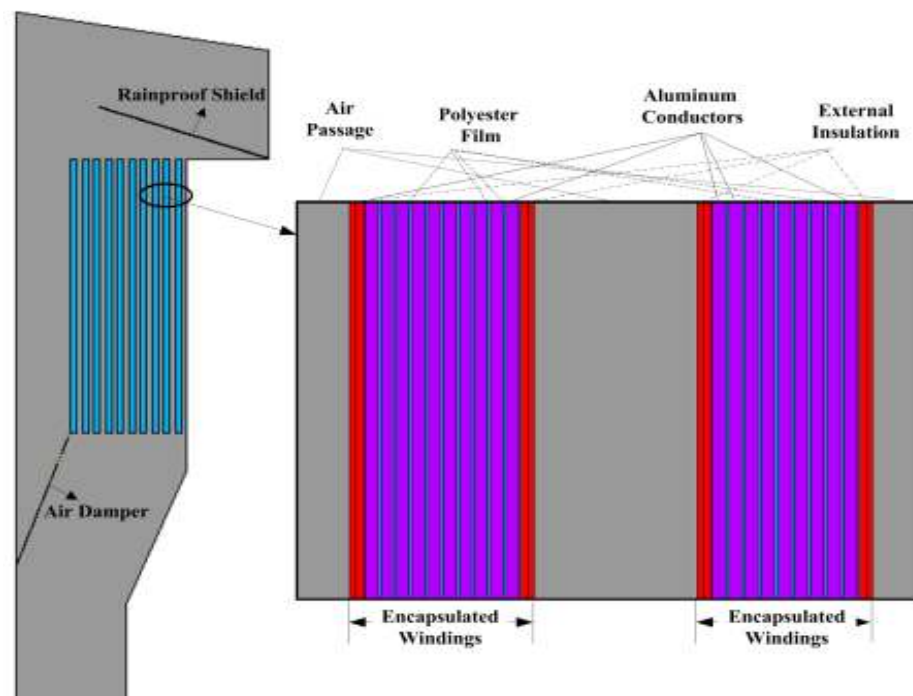


Fig. 2: The calculation model of reactor

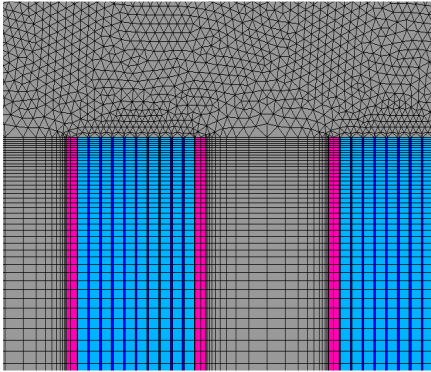


Fig. 3: Partial FE model

Table 1: Main geometry and material properties of the model

Material	Thermal conductivity (W/(m·K))	Width (mm)
Aluminum conductor	217.7	Different diameter in each layer
DMD	0.3	0.92
Polyester film	0.3	0.20
Glass fiber dipped by epoxy	0.5	1.2

model is established, as shown in Fig. 3. The total elements and nodes are 371,550 and 268,051. Table 1 describes the main geometrical and material properties of the analyzed model.

The thermal field and fluid field are coupled directly according to Navier-Stokes equations. Firstly, coupled magnetic field-circuit calculation is carried out, then, the Joule heat is obtained. Secondly, the Joule heat is coupled into the thermal field as heat generation rate, in addition to some other proper fluid and thermal boundary conditions, the thermal field and fluid field is simultaneously calculated. Proper boundary conditions should be set as followings.

- Set non-slip boundary condition ( $v_x = 0, v_y = 0$ ) on the surface of reactor
- Set surrounding temperature (here 20°C in accordance with normal temperature)

Table 2: The heat generation rate of every aluminum conductor in each encapsulated winding (W/m<sup>3</sup>)

No	Layer of aluminum conductor										
	1	2	3	4	5	6	7	8	9	10	11
1	6774	7354	8770	9408	11126	14907	21413	31591	47433	70667	90953
2	39294	49537	43073	41736	51493	51638	54563	66352			
3	56514	54328	55826	59018	63115	67655	73971	84237	102199	156779	
4	109927	93485	83859	80494	78931	77781	79337	117892			
5	70354	64273	62233	77165	80622	82942	86393	93942	108894	135896	
6	91265	95927	84969	82176	80014	79210	79116	83281	97536		
7	99423	88118	84872	85429	86136	87427	90638	99401	119674		
8	110638	90188	80798	77544	75920	75025	74228	75184	80655	95083	
9	92743	76529	69104	66349	65593	65323	65099	66388	71109	82933	
10	80841	52437	34607	23745	17542	14223	12518	11617	10960		

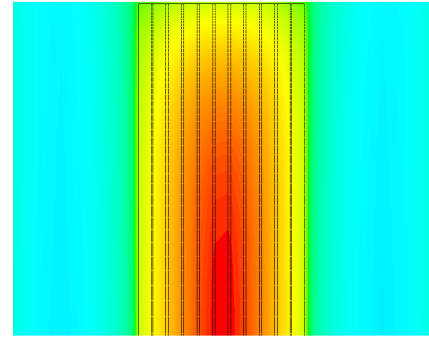


Fig. 4: The hottest temperature of the encapsulated winding

- Set reference pressure to zero at the node in air outlet
- Set axisymmetric boundary condition ( $v_x = 0$ ) at the node on axis
- Set radiative heat transfer boundary conditions for the surfaces of shielding and encapsulated windings. Set Stefan-Boltzman constant to 5.67e-8 and temperature offset to 273. Here all the emissivity is set to 0.9.

### CALCULATION RESULTS AND ANALYSIS

After coupled magnetic field-circuit analysis, the Joule's losses can be calculated. Table 2 gives the losses of every aluminum conductor in each encapsulated winding.

In forced air cooling reactor, the cooling air blows from bottom to top and flows through the air passages between two encapsulated windings. From Fig. 4, the temperature distribution in one encapsulated winding is non uniform because the heat conductivity of insulation material is much smaller than that of aluminum conductor.

From Fig. 5, we can find that the flow velocity of air in passage between encapsulated windings, which are near the outside and inside wall, is faster. Therefore, the hottest point is on the encapsulated winding in middle of model, as shown in Fig. 6.

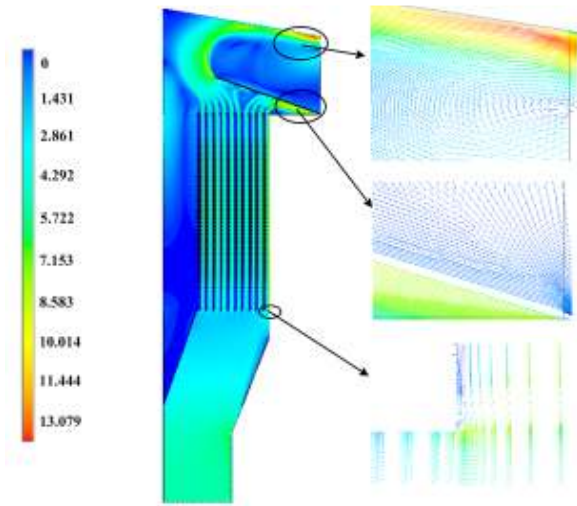


Fig. 5: Air velocity distribution and partial vector velocity

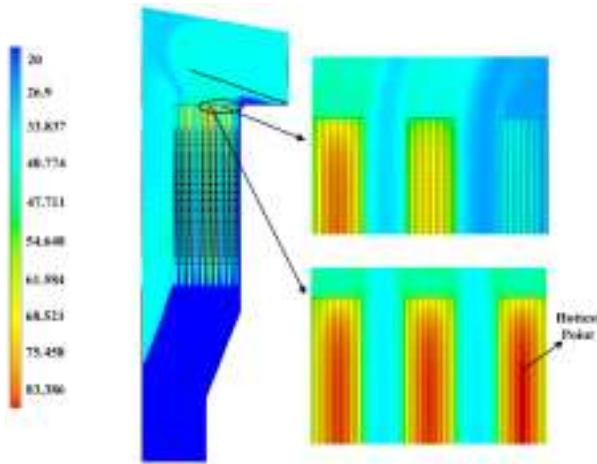


Fig. 6: The temperature distributions in reactor

The rainproof shield has an important influence on the air velocity among the encapsulated windings. Thus, the air cooling should be considered in the design of rainproof shield. The uniform temperature rise distribution might be achieved by improvement of the geometrical structure of rainproof shield.

### CONCLUSION

In this study, the temperature rise of a forced air cooling dry-type air-core reactor is calculated by finite element method for coupled magnetic-thermal-fluid field. The current distribution among the encapsulated windings is analyzed by using coupled magnetic field-circuit method. The temperature rise distribution of reactor is tightly related with current Joule's losses in each encapsulated windings, the thermal parameters of

insulation materials and the structures of diverse components in reactor, such as rainproof shield which may influence on the air flow among the encapsulated windings.

### ACKNOWLEDGMENT

This study is supported by National Natural Science Foundation of China (No. 51207081).

### REFERENCES

- Ho, S.L., Y. Li, X. Lin, H.C. Wong and K.W.E. Cheng, 2006. A 3-D study of eddy current field and temperature rises in a compact bus duct system. *IEEE T. Magn.*, 42(4): 987-990.
- Ho, S.L., Y. Li, X. Lin, E. Lo, K.W.E. Cheng, *et al.*, 2007. Calculations of eddy current, fluid and thermal fields in an air insulated bus duct system. *IEEE T. Magn.*, 43(4): 1433-1436.
- IEEE Std., 1996. C57.16-1996-IEEE Standard Requirements, Terminology and Test Code for Dry-Type Air-Core Series-Connected Reactors. Transformers Committee of the IEEE Power Engineering Society, DOI: 10.1109/ IEEESTD. 1997. 82418.
- Liu, J., 1991. Adaptive Finite Element Method and Temperature Field Calculation for Reactor. Xi'an Jiaotong University, Xi'an, China.
- Liu, Z., Y. Geng, J. Wang and D.W.A. Chen, 2003. Design and analysis of new type air-core reactor based on coupled fluid-thermal field calculation. *Diangong Jishu Xuebao T. China Electrotech. Soc.*, 18(6): 59-63.
- Wu, S., D. Wu and S. Yan, 1997. A study of design and calculation method for dry-type reactor with air core. *Transformer*, 34(3): 18-22.
- Wu, A., D. Chen, J. Wang, B. Cai and Y. Geng, 2002. Evaluation of thermal performance for air-insulated busbar trunking system by coupled magneto-fluid-thermal fields. *Proceeding of International Conference on Power System Technology*, 4: 2159-2163, DOI: 10.1109/ICPST.2002.1047164.
- Zhang, Y., J. Ruan, T. Huang, X. Yang, H. Zhu, *et al.*, 2012a. Calculation of temperature rise in air-cooled induction motors through 3-D coupled electromagnetic fluid-dynamical and thermal finite-element analysis. *IEEE T. Magn.*, 48(2): 1047-1050.
- Zhang, Y., X. Huang, T. Huang, J. Ruan and X. Wu, 2012b. Ventilation structure improvement of air-cooled induction motor using multiphysics simulations. *Telkomnika*, 10(3): 451-458.